Kinetics of Bromide Oxidation by (Oxalato)oxodiperoxomolybdate(VI)

Martha S. Reynolds,* Steven J. Morandi, James W. Raebiger, Sean P. Melican, and Sean P. E. Smith

Department of Chemistry, Colgate University, Hamilton, New York 13346

Received April 13, 1994[⊗]

The kinetics of bromide oxidation by (oxalato)oxodiperoxomolybdate(VI), $MoO(O_2)_2(C_2O_4)^{2-}$, were studied. At 25 °C and pH 5.0, the reaction obeys the rate law $d[Br^+]/dt = k_{Br}[MoO(O_2)_2(C_2O_4)^{2-}][Br^-]$, where $k_{Br} = (4.8 \pm 0.4) \times 10^{-3}\ M^{-1}\ s^{-1}$, measured by the production of bromophenol blue from phenol red. The latter reaction was previously used for bromine analysis and as an assay for bromoperoxidase enzyme activity; we now employ it to quantify the initial rate of bromine production at pH 5.0. The oxidation of bromide by $MoO(O_2)_2(C_2O_4)^{2-}$ is catalytic in the presence of excess hydrogen peroxide and bromide. We propose a mechanism that involves the interaction of $MoO(O_2)_2(C_2O_4)^{2-}$ and bromide to yield Br^+ and a monoperoxo intermediate, $MoO_2(O_2)(C_2O_4)^{2-}$; the monoperoxo complex combines with hydrogen peroxide to regenerate the initial diperoxo complex or undergoes hydrolysis to yield the final molybdenum product, $MoO_3(C_2O_4)^{2-}$. The primary bromine product is unknown; "Br^+" represents an equilibrium mixture of hypobromous acid, hypobromite, bromine, and tribromide. In the absence of an organic substrate, dioxygen is produced from the oxidation of hydrogen peroxide by Br^+. The aqueous chemistry of the vanadium(V) and tungsten(VI) analogues is not well defined. Neither $VO(O_2)_2(C_2O_4)^{3-}$ nor $WO(O_2)_2(C_2O_4)^{2-}$ was obtained as the sole species in solution at pH 5.0. The monoperoxo bis(oxalato) complex $VO(O_2)(C_2O_4)_2^{3-}$ reacted with bromide at a rate indistinguishable from that of the uncatalyzed case at pH 5.0 and 25 °C. The diperoxo tungsten complex $WO(O_2)_2(C_2O_4)^{2-}$ reacted with bromide at a rate faster than that for its molybdenum(VI) counterpart, but a complete kinetic analysis was precluded by the presence of the unchelated complex $WO(OH)(O_2)_2(H_2O)^-$.

Introduction

Metal complexes containing the peroxide ligand are efficient oxidizing agents for numerous substrates, including olefins, arenes, alcohols, phosphines, sulfides, and halides.[1,2] A vanadium−peroxo species is a likely intermediate in the mechanism of vanadium bromoperoxidase (VBrPO),[3−6] which employs hydrogen peroxide and bromide in the bromination of an organic substrate (eq 1).

$$RH + H_2O_2 + Br^- + H^+ \rightarrow RBr + 2H_2O \qquad (1)$$

The mechanism apparently comprises the reaction of the enzyme with hydrogen peroxide and bromide,[7,8] during which an enzyme−peroxide intermediate is formed.[9] Bromination of an organic substrate may occur by direct interaction of the substrate with an enzyme-trapped brominating equivalent[10] or after release of "Br^+" from the enzyme. The primary bromine product is unknown because an equilibrium mixture of HOBr, OBr^-, Br_2, and Br_3^- is rapidly obtained.

Because the intermediate enzyme−peroxide species is likely a peroxo complex of vanadium(V), we seek to identify synthetic peroxometal complexes that are capable of oxidizing bromide, to probe the mechanistic details of such chemistry, and to understand the features that enhance the reactivity of peroxometal complexes toward bromide.

The work of several groups is pertinent. A variety of peroxo complexes of vanadium(V) and molybdenum(VI) were prepared and characterized in the laboratories of Mimoun,[11,12] Djordjevic,[13−16] Griffith,[17−21] Stomberg,[22−24] Einstein,[25,26] and Mares.[27] These complexes typically contain a bi- or tridentate hetero ligand, an apical oxo ligand, and one or two peroxide

[⊗] Abstract published in *Advance ACS Abstracts,* September 15, 1994.

(1) Mimoun, H. In *The Chemistry of Peroxides*; Patai, S., Ed.; Wiley: New York, 1983; Chapter 15.
(2) Sheldon, R. A.; Kochi, J. K. *Metal-Catalyzed Oxidations of Organic Compounds*; Academic: New York, 1981; Chapter 4, pp 71−119.
(3) Wever, R.; Krenn, B. E. In *Vanadium in Biological Systems*; Chasteen, N. D., Ed.; Kluwer Academic Publishers: Boston, 1990; Chapter V, pp 81−97.
(4) Wever, R.; Kustin, K. *Adv. Inorg. Chem.* **1990**, *35*, 81−115.
(5) Rehder, D. *Angew. Chem., Int. Ed. Engl.* **1991**, *30*, 148−167.
(6) Butler, A.; Carrano, C. J. *Coord. Chem. Rev.* **1991**, *109*, 61−105.
(7) de Boer, E.; Wever, R. *J. Biol. Chem.* **1988**, *263*, 12326−12332.
(8) Everett, R. R.; Soedjak, H. S.; Butler, A. *J. Biol. Chem.* **1990**, *265*, 15671−15679.
(9) Tromp, M. G. M.; Olafsson, G.; Krenn, B. E.; Wever, R. *Biochim. Biophys. Acta* **1990**, *1040*, 192−198.
(10) Tschirret-Guth, R. A.; Butler, A. *J. Am. Chem. Soc.* **1994**, *116*, 411−412.
(11) Mimoun, H.; Seree de Roch, I.; Sajus, L. *Bull. Soc. Chim. Fr.* **1969**, 1481−1492.
(12) Mimoun, H.; Saussine, L.; Daire, E.; Postel, M.; Fischer, J.; Weiss, R. *J. Am. Chem. Soc.* **1983**, *105*, 3101−3110.
(13) Djordjevic, C.; Craig, S. A.; Sinn, E. *Inorg. Chem.* **1985**, *24*, 1281−1283.
(14) Djordjevic, C.; Covert, K. J.; Sinn, E. *Inorg. Chim. Acta* **1985**, *101*, L37−L39.
(15) Djordjevic, C.; Puryear, B. C.; Vuletic, N.; Abelt, C. J.; Sheffield, S. J. *Inorg. Chem.* **1988**, *27*, 2926−2932.
(16) Djordjevic, C.; Lee, M.; Sinn, E. *Inorg. Chem.* **1989**, *28*, 719−723.
(17) Campbell, N. J.; Capparelli, M. V.; Griffith, W. P.; Skapski, A. C. *Inorg. Chim. Acta* **1983**, *77*, L215−L216.
(18) Flanagan, J.; Griffith, W. P.; Skapski, A. C.; Wiggins, R. W. *Inorg. Chim. Acta* **1985**, *96*, L23−L24.
(19) Dengel, A. C.; Griffith, W. P.; Powell, R. D.; Skapski, A. C. *J. Chem. Soc., Chem. Commun.* **1986**, 555−556.
(20) Dengel, A. C.; Griffith, W. P.; Powell, R. D.; Skapski, A. C. *J. Chem. Soc., Dalton Trans.* **1987**, 991−995.
(21) Campbell, N. J.; Dengel, A. C.; Edwards, C. J.; Griffith, W. P. *J. Chem. Soc., Dalton Trans.* **1989**, 1203−1208.
(22) Stomberg, R. *Acta Chem. Scand.* **1970**, *24*, 2024−2036.
(23) Szentivanyi, H.; Stomberg, R. *Acta Chem. Scand.* **1983**, *A37*, 709−714.
(24) Stomberg, R. *Acta Chem. Scand.* **1986**, *A40*, 168−176.
(25) Drew, R. E.; Einstein, F. W. B. *Inorg. Chem.* **1973**, *12*, 829−835.
(26) Begin, D.; Einstein, F. W. B.; Field, J. *Inorg. Chem.* **1975**, *14*, 1785−1790.

0020-1669/94/1333-4977$04.50/0

ligands coordinated in an η^2 fashion in the equatorial plane of the metal ion. Thompson and co-workers examined the aqueous chemistry of several peroxovanadium(V) and peroxomolybdenum(VI) complexes, including the kinetics of oxidation by these complexes of a coordinated thiolate ligand, $Co(en)_2(SCH_2CH_2NH_2)^{2+}$ (en = ethylenediamine).[28-30] Several other studies are relevant to metal-mediated halide oxidation by hydrogen peroxide because a peroxometal intermediate is observed. Butler and co-workers demonstrated the catalytic mediation of an oxovanadium(V) complex of a Schiff-base ligand in the oxidation of bromide by hydrogen peroxide.[31] Secco studied the kinetics of iodide oxidation by hydrogen peroxide in the presence of vanadate ion,[32-34] Arias et al. examined the analogous system for molybdate ion,[35] Butler extended the chemistry of vanadate, molybdate, and tungstate ions to include the catalytic oxidation of bromide,[36,37] and Herrmann[38] and Espenson[39] showed that bromide oxidation catalyzed by methylrhenium trioxide involves peroxorhenium intermediates. However, a detailed kinetics analysis of the oxidation of bromide by a peroxo complex containing chelating ligands has not previously been realized.

We find (oxalato)oxodiperoxomolybdate(VI), $MoO(O_2)_2(C_2O_4)^{2-}$, to be an effective catalyst in the oxidation of bromide by hydrogen peroxide. An early synthesis of this complex[40,41] was later improved;[20] the crystal structure of the potassium salt is available;[14,22] and certain aspects of the aqueous chemistry are now known, including its reactivity in the oxidation of the sulfur atom in $Co(en)_2(SCH_2CH_2NH_2)^{2+}$.[29]

In this report of catalytic bromide oxidation by a chelated peroxometal species, we describe the kinetics of the reaction between bromide and $MoO(O_2)_2(C_2O_4)^{2-}$ and propose a mechanism for the catalytic process.

Experimental Section

Materials and Solutions. Potassium (oxalato)oxodiperoxomolybdate(VI), $K_2[MoO(O_2)_2(C_2O_4)]$,[20] potassium (oxalato)trioxomolybdate(VI), $K_2[MoO_3(C_2O_4)]$,[42] potassium (oxalato)oxodiperoxovanadate(V), $K_3[VO(O_2)_2(C_2O_4)]$,[43,44] and potassium bis(oxalato)oxoperoxovanadate(V), $K_3[VO(O_2)(C_2O_4)_2]$,[44] were prepared by literature methods. Solutions of $VO(O_2)_2(H_2O)_2^-$ for investigation by ^{51}V NMR spectroscopy were prepared by combining NH_4VO_3 (5 mM) with H_2O_2 (10 mM) in 0.040 M acetate buffer (pH 5.0). Lithium bromide (>97%) was obtained from Fluka. Lithium perchlorate was prepared by the neutralization of lithium carbonate (>99%, Fluka) with perchloric acid and was recrystallized three times. Potassium molybdate (Aldrich), potassium tungstate (Aldrich), phenol red (4,4′-(3*H*-2,1-benzoxathiol-3-ylidene)bis(phenol) *S*,*S*-dioxide) (Fisher), phenol red sodium salt (Matheson, Coleman, and Bell), and bromophenol blue (4,4′-(3*H*-2,1-benzoxathiol-3-ylidene)bis(2,6-dibromophenol) *S*,*S*-dioxide) (Fisher) were used as received. Distilled water was purified with a Barnstead Nanopure deionizer. Solutions of hydrogen peroxide were standardized by iodometric titration or by spectrophotometric measurement of chloroperoxidase-catalyzed triiodide formation, a modification of the method of Cotton and Dunford.[45]

Stock solutions of bromine were prepared by dissolution of Br_2 in 0.10 M NaOH and were standardized spectrophotometrically by the oxidation of iodide to triiodide (λ_{max} = 353 nm, ϵ = 26 400 M^{-1} cm^{-1} for I_3^-).[46] A calibration curve for the dependence of bromophenol blue absorbance on bromine concentration was prepared by combining bromine with phenol red and bromide in oxalate or acetate buffer (0.010 M buffer, pH 5.0). The ionic strength was adjusted to 1.0 M with lithium perchlorate. The absorbance of each solution was measured at 588 nm, the λ_{max} for bromophenol blue. The value of $dA/d[Br^+]$ was obtained from the slope of a plot of A vs $[Br^+]$. Essentially identical results were obtained for acetate and oxalate buffer and for bromide concentrations of 25 and 500 mM.

The stability of 1 mM $MoO(O_2)_2(C_2O_4)^{2-}$ in the presence of 1 mM H_2O_2 (0.010 M oxalate buffer, pH 5.0, ionic strength 1.0 M) was confirmed by monitoring the UV/visible spectrum for 28 h at 25 °C; no change in absorbance was observed.

Kinetics Measurements. The reaction of $MoO(O_2)_2(C_2O_4)^{2-}$ with Br^- was monitored by (1) the disappearance of the metal complex and (2) the production of bromine as manifested by the bromination of phenol red to bromophenol blue. The oxidation of bromide by tungstate in the presence of hydrogen peroxide and oxalate anion was monitored by the latter method. Spectral changes for metal-catalyzed reactions were followed at 25.0 ± 0.5 °C with a Hewlett-Packard 8452A diode array spectrophotometer. Conventional mixing techniques were employed for monitoring the disappearance of $MoO(O_2)_2(C_2O_4)^{2-}$. In the case of bromophenol blue production, a stopped-flow mixing device (Hi-Tech SFA-12 Rapid Kinetics Accessory) was used in conjunction with the diode array spectrophotometer.

Disappearance of $MoO(O_2)_2(C_2O_4)^{2-}$. In a typical experiment, a solution of $MoO(O_2)_2(C_2O_4)^{2-}$ and hydrogen peroxide was mixed with an equal volume of a solution of lithium bromide. Both solutions contained 0.010 M oxalate buffer (pH 5.0) and sufficient lithium perchlorate to maintain the ionic strength at 1.0 M. Initial concentrations after mixing were 1 mM $MoO(O_2)_2(C_2O_4)^{2-}$, 1−10 mM H_2O_2, and 0.025−0.400 M LiBr. Hydrogen peroxide was required to maintain $MoO(O_2)_2(C_2O_4)^{2-}$ in the diperoxo form at the start of the reaction. For hydrogen peroxide concentrations in excess of 1 mM, an oxalate buffer concentration of 0.10 M was employed. Reaction systems were monitored spectrophotometrically over the wavelength range 250−450 nm. Data analysis was performed at 320 nm, the λ_{max} for $MoO(O_2)_2(C_2O_4)^{2-}$.[29] Pseudo-first-order rate constants were determined from nonlinear least-squares fits to the equation $(A - A_\infty) = \alpha \exp(-k_{obs}t)$ or from the slopes of plots of $-\ln(A - A_\infty)$ vs t. In the latter instance, all plots were linear for at least 4 half-lives.

Metal-Catalyzed Formation of Bromine. The formation of bromine by the metal-catalyzed oxidation of bromide was monitored by the production of bromophenol blue, the tetrabromination product of phenol red.[47,48] Solutions were prepared and mixed as described above for monitoring the metal complex, except that phenol red (10−50 μM after mixing) was included in the metal-containing solution. The $MoO(O_2)_2(C_2O_4)^{2-}$ concentration was varied over the range of 0.1−1 mM after mixing, and the hydrogen peroxide concentration was at least equimolar to $MoO(O_2)_2(C_2O_4)^{2-}$. Reactions were monitored spectrophotometrically over the wavelength range 350−750 nm. Data

(27) Jacobson, S. E.; Tang, R.; Mares, F. *Inorg. Chem.* **1978**, *17*, 3055−3063.
(28) Ghiron, A. F.; Thompson, R. C. *Inorg. Chem.* **1988**, *27*, 4766−4771.
(29) Ghiron, A. F.; Thompson, R. C. *Inorg. Chem.* **1989**, *28*, 3647−3650.
(30) Ghiron, A. F.; Thompson, R. C. *Inorg. Chem.* **1990**, *29*, 4457−4461.
(31) Clague, M. J.; Keder, N. L.; Butler, A. *Inorg. Chem.* **1993**, *32*, 4754−4761.
(32) Secco, F.; Celsi, S.; Grati, C. *J. Chem. Soc., Dalton Trans.* **1972**, 1675−1678.
(33) Celsi, S.; Secco, F.; Venturini, M. *J. Chem. Soc., Dalton Trans.* **1974**, 793−795.
(34) Secco, F. *Inorg. Chem.* **1980**, *19*, 2722−2725.
(35) Arias, C.; Mata, F.; Perez-Benito, J. F. *Can. J. Chem.* **1990**, *68*, 1499−1503.
(36) de la Rosa, R. I.; Clague, M. J.; Butler, A. *J. Am. Chem. Soc.* **1992**, *114*, 760−761.
(37) Meister, G. E.; Butler, A. *Inorg. Chem.* **1994**, *33*, 3269−3275.
(38) Herrmann, W. A.; Fischer, R. W.; Scherer, W.; Rauch, M. U. *Angew. Chem., Int. Ed. Engl.* **1993**, *32*, 1157−1160.
(39) Espenson, J. H.; Pestovsky, O.; Huston, P.; Staudt, S. *J. Am. Chem. Soc.* **1994**, *116*, 2869−2877.
(40) Mazzucchelli, A. *Atti. Accad. Naz., Lincei Cl. Sci. Fis., Mat. Nat. Rend.* **1907**, *16*, 963.
(41) Mazzucchelli, A.; Zangrilli, G. *Gazz. Chim. Ital.* **1910**, *40*, 49.
(42) Rosenheim, A. *Chem. Ber.* **1893**, *26*, 1191−1194.
(43) Vuletic, N.; Djordjevic, C. *J. Chem. Soc., Dalton Trans.* **1973**, 1137−1141.
(44) Schwendt, P.; Petrovic, P.; Uskert, D. *Z. Anorg. Allg. Chem.* **1980**, *466*, 232−236.
(45) Cotton, M. L.; Dunford, H. B. *Can. J. Chem.* **1973**, *51*, 582−587.
(46) Thompson, R. C. *Adv. Inorg. Bioinorg. Mech.* **1986**, *4*, 65−106.
(47) Péron, A.; Courtot-Coupez, J. *Analusis* **1978**, *6*, 389−394.
(48) de Boer, E.; Plat, H.; Tromp, M. G. M.; Wever, R.; Franssen, M. C. R.; van der Plas, H. C.; Meijer, E. M.; Schoemaker, H. E. *Biotechnol. Bioeng.* **1987**, *30*, 607−610.

analysis was performed at 588 nm, the λ_{max} for bromophenol blue. Initial rates dA_{588}/dt for each reaction were measured from the slope of the steady-state portion of the absorbance vs time trace. Two or three replicate determinations were averaged for each concentration. Absolute rates $d[Br^-]/dt$ were obtained by application of the reciprocal of the factor $dA/d[Br^-]$ defined above to the experimental rates dA_{588}/dt. Control experiments revealed no reaction between $MoO(O_2)_2(C_2O_4)^{2-}$ and phenol red in the absence of bromide or between phenol red and bromide in the absence of the molybdenum complex.

In a limited study, the reactivity of $MoO(OH)(O_2)_2(H_2O)^-$ with bromide in the presence of hydrogen peroxide and phenol red was investigated. Initial concentrations after mixing were 0.04−1 mM K_2MoO_4, 0.033−0.500 M H_2O_2, 0.049−0.500 M LiBr, and 45 μM phenol red in 0.010 M acetate buffer at pH 5.0. The reactivity of tungstate (0.1 mM K_2WO_4) with H_2O_2 (20 mM) and LiBr (0.010−0.400 M) in the presence of phenol red (45 μM) in 0.010 M oxalate buffer (pH 5.0) and in 0.010 M acetate buffer (pH 5.0) was studied in a similar fashion. The ionic strength was adjusted to 1.0 M with $LiClO_4$ in all cases.

Uncatalyzed Bromide Oxidation. The rate of uncatalyzed bromide oxidation by hydrogen peroxide was determined by mixing a solution of H_2O_2 and phenol red with bromide solution. The reaction solutions contained 4.5×10^{-5} M phenol red, 10−100 mM H_2O_2, and 0.010−0.200 M LiBr in 0.010 M acetate buffer (pH 5.0) immediately after mixing. Ionic strength was maintained at 1.0 M with lithium perchlorate. To avoid catalysis by adventitious metal ions, glassware was rinsed with 10 mM EDTA and deionized water before use, and 10 μM EDTA was included in the reaction solutions.

Product Yield. The production of bromophenol blue from the bromination of phenol red was employed to quantify the bromine produced in the reaction of $MoO(O_2)_2(C_2O_4)^{2-}$ with excess hydrogen peroxide and bromide. The sodium salt of phenol red was required in order to obtain sufficiently high concentrations of the substrate. The reaction was initiated by combining a buffered solution of $MoO(O_2)_2(C_2O_4)^{2-}$, hydrogen peroxide, and phenol red with an equal volume of a buffered solution of bromide. Initial concentrations after mixing were 1.0 mM $MoO(O_2)_2(C_2O_4)^{2-}$, 5.0 mM H_2O_2, 1.9×10^{-5} M phenol red, 1.0 M LiBr, and 0.040 M oxalate buffer (pH 5.0). The absorbance was measured at 588 nm after 80-fold dilution of the reaction solution in 0.010 M oxalate buffer (pH 5.0).

Oxygen Evolution. Dioxygen production was measured at 25 °C with a Yellow Springs Instruments Clark-type electrode (YSI 5331) and monitor (YSI 5300). The instrument was calibrated against air-saturated water, which has an oxygen concentration of 0.2445 mM at 25 °C.[49] A solution containing MoO_4^{2-}, LiBr, and oxalate buffer was purged with N_2 before measurement. The reaction was initiated by the addition of a small volume of hydrogen peroxide solution. Initial rates of O_2 production were determined from solutions initially containing 67 μM MoO_4^{2-}, 0.033 M LiBr, 2−4 mM H_2O_2, and 0.010 M oxalate buffer (pH 5.0). Quantitation of total O_2 production was accomplished with solutions initially containing 67 μM MoO_4^{2-}, 2.0 M LiBr, 0.4 mM H_2O_2, and 0.010 M oxalate buffer (pH 5.0).

^{51}V NMR Spectroscopy. Vanadium-51 NMR spectroscopy was employed to investigate the nature of $VO(O_2)_2(C_2O_4)^{3-}$ and $VO(O_2)(C_2O_4)_2^{3-}$ in aqueous solution in the presence of hydrogen peroxide and oxalate buffer. Solutions of 1−10 mM V complex were examined at 25 °C in 10 mm tubes on a General Electric GN300 spectrometer at 79 MHz. The pulse width was 20 μs, and the relaxation delay was 100 ms. Signals were referenced to $VOCl_3$ (0 ppm), which was employed as an external standard. Authentic samples of $VO(O_2)_2(H_2O)_2^-$ and $VO(O_2)(C_2O_4)_2^{3-}$ gave signals at −690 and −597 ppm, respectively, at pH 5.0.

Results

Disappearance of $MoO(O_2)_2(C_2O_4)^{2-}$. When $MoO(O_2)_2(C_2O_4)^{2-}$ and 1 equiv of hydrogen peroxide were combined with excess bromide in oxalate buffer at pH 5.0, a decrease in the characteristic absorbance maximum of $MoO(O_2)_2(C_2O_4)^{2-}$ at 320 nm was observed. Figure 1 depicts this transformation

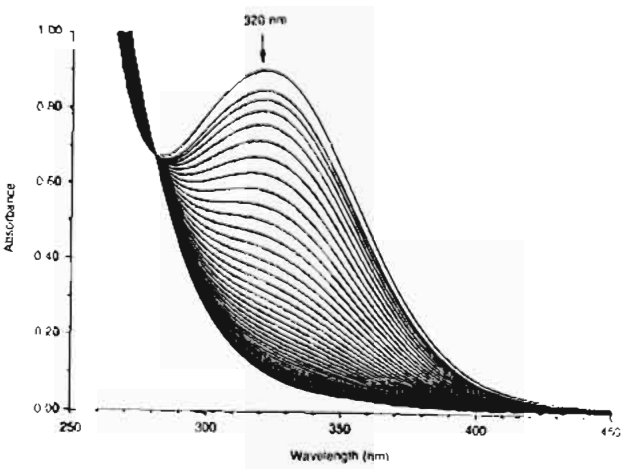

Figure 1. Spectral changes at 15 min intervals for the reaction of $MoO(O_2)_2(C_2O_4)^{2-}$, H_2O_2, and Br^- at 25 °C. Initial concentrations: 1 mM $MoO(O_2)_2(C_2O_4)^{2-}$; 1 mM H_2O_2; 0.025 M LiBr; 0.010 M oxalate buffer (pH 5.0); 1.0 M ionic strength.

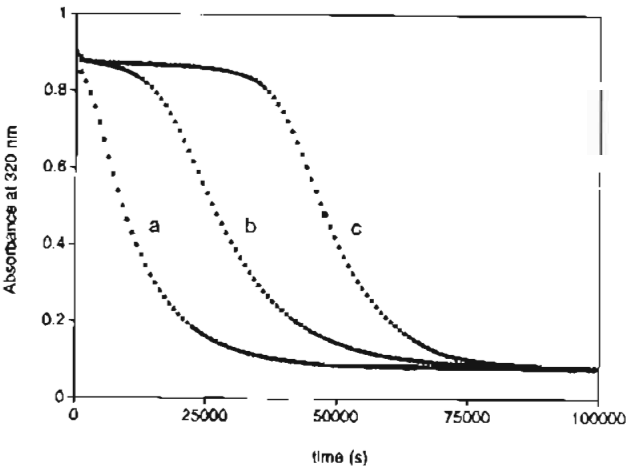

Figure 2. Plot of the time dependence of absorbance at 320 nm for reaction of $MoO(O_2)_2(C_2O_4)^{2-}$, Br^-, and varying H_2O_2 concentrations at 25 °C. Initial concentrations: 1 mM $MoO(O_2)_2(C_2O_4)^{2-}$; 0.025 M LiBr; 1 mM (a), 5 mM (b), and 10 mM (c) H_2O_2; 0.010 M (a) and 0.10 M (b, c) oxalate buffer (pH 5.0); 1.0 M ionic strength.

under conditions of 1 mM $MoO(O_2)_2(C_2O_4)^{2-}$, 1 mM H_2O_2, 0.025 M LiBr, 0.010 M oxalate buffer, and an ionic strength of 1.0 M ($LiClO_4$). An isosbestic point at 281 nm is apparent. The final spectrum is identical with that of an authentic sample of $MoO_3(C_2O_4)^{2-}$ in pH 5.0 oxalate buffer. The time dependence of the absorbance at 320 nm for this experiment is given in Figure 2a, where an initial lag is followed by an exponential decay. A plot of $-\ln|A - A_\infty|$ vs time for the latter part of the reaction is linear for more than 4 half-lives, indicating that the process is first-order in the $MoO(O_2)_2(C_2O_4)^{2-}$ complex. The slope of the plot gives k_{obs}. The experiment was repeated for a series of bromide concentrations up to 400 mM, and the resulting plot of k_{obs} vs. $[Br^-]$ is shown in Figure 3. The first-order dependence on bromide concentration is apparent from the linearity of the plot, and the overall second-order rate law for the disappearance of the $MoO(O_2)_2(C_2O_4)^{2-}$ complex is given in eq 2. The rate constant $k_{Mo} = (2.3 \pm 0.1) \times 10^{-3}$ M^{-1} s^{-1} was obtained from the slope of the plot in Figure 3. The uncertainty is expressed as the standard deviation of the slope.

$$-d[MoO(O_2)_2(C_2O_4)^{2-}]/dt = k_{Mo}[MoO(O_2)_2(C_2O_4)^{2-}][Br^-] \quad (2)$$

(49) *YSI Model 5300 Biological Oxygen Monitor Instruction Manual*; Yellow Springs Instrument Co., Inc.: Yellow Springs, OH; p 13.

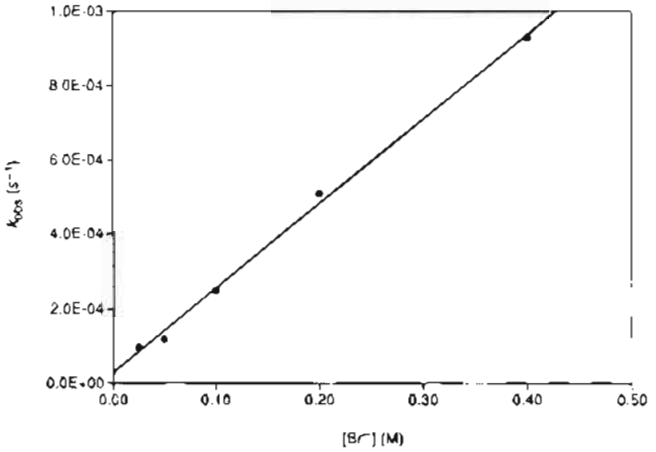

Figure 3. Plot of observed rate constants for the reaction of $MoO(O_2)_2(C_2O_4)^{2-}$, H_2O_2, and Br^- at 25 °C as a function of bromide concentration. Initial concentrations: 1 mM $MoO(O_2)_2(C_2O_4)^{2-}$; 1 mM H_2O_2; 0.025–0.400 M LiBr; 0.010 M oxalate buffer (pH 5.0); 1.0 M ionic strength. The slope of the line is $k_{Br^-} = (2.3 \pm 0.1) \times 10^{-3}$ M^{-1} s^{-1}.

For a constant initial hydrogen peroxide concentration, the initial lag in the absorbance vs time trace was increasingly short-lived as the bromide concentration was increased (data not shown). Increasing the initial hydrogen peroxide concentration increased the length of the initial lag phase, as depicted in Figure 2 for H_2O_2 concentrations of 1 (a), 5 (b), and 10 mM (c), with 1 mM $MoO(O_2)_2(C_2O_4)^{2-}$ and 0.025 M LiBr. The experiments were conducted in both 0.010 and 0.100 M oxalate buffer (pH 5.0). For the higher hydrogen peroxide concentrations, a shift in the absorption maximum of the molybdenum complex from 320 to 310 nm was observed over the course of the reaction in 0.010 M but not in 0.100 M oxalate buffer. Such a shift is indicative of the conversion of $MoO(O_2)_2(C_2O_4)^{2-}$ to $MoO(OH)(O_2)_2(H_2O)^-$.[29] Similar experiments employing high hydrogen peroxide concentrations in a mixed-buffer system of 0.010 M oxalate and 0.500 M acetate (pH 5.0) did not produce a shift in the absorption maximum. We conclude that the shift was due to the loss of buffering capacity and not to the consumption of oxalate ligand.

As noted above, an isosbestic point exists at 281 nm in the time-dependent spectra of Figure 1 under conditions of 1 mM $MoO(O_2)_2(C_2O_4)^{2-}$, 1 mM H_2O_2, and 0.025 M LiBr. As the initial bromide concentration was increased in successive experiments, the isosbestic point apparent at the beginning of the reaction persisted for increasingly short times. At the highest bromide concentrations employed, no isosbestic point was observed, but an intense absorption feature at 266 nm characteristic of tribromide[46] appeared and then slowly disappeared, consistent with the production of O_2 by the oxidation of hydrogen peroxide (see below). The effect of the reaction conditions on the longevity of the initial lag, on the isosbestic point, and on the transient tribromide species is interpreted below in terms of a proposed mechanism.

Addition of hydrogen peroxide (10 mM) to a spent reaction mixture yielded the spectrum of the $MoO(O_2)_2(C_2O_4)^{2-}$ complex, followed by a decay similar to that in Figure 2c, as the complex reacted with excess bromide in solution.

Formation of Bromophenol Blue. The bromination of phenol red to bromophenol blue was employed to follow the rate of bromine production by the $MoO(O_2)_2(C_2O_4)^{2-}$ system. Figure 4 is representative of the rapid spectral changes that occurred when phenol red was included in a reaction mixture of $MoO(O_2)_2(C_2O_4)^{2-}$, 1 equiv of hydrogen peroxide, and a pseudo-first-order excess of bromide in 0.010 M oxalate buffer

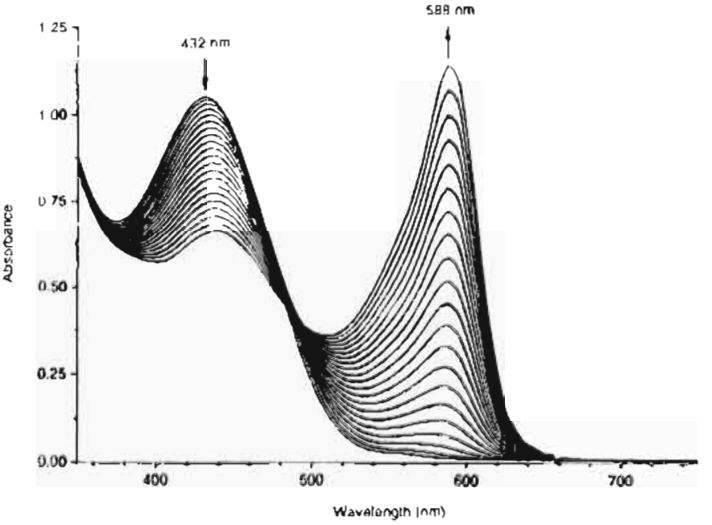

Figure 4. Spectral changes at 40 s intervals for the formation of bromophenol blue in the reaction of $MoO(O_2)_2(C_2O_4)^{2-}$, H_2O_2, Br^-, and phenol red at 25 °C. Initial concentrations: 1 mM $MoO(O_2)_2(C_2O_4)^{2-}$; 1 mM H_2O_2; 0.025 M LiBr; 4.5×10^{-5} M phenol red; 0.010 M oxalate buffer (pH 5.0); 1.0 M ionic strength.

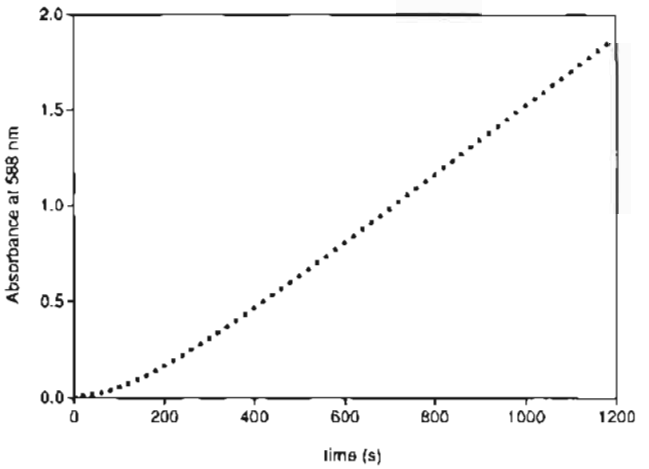

Figure 5. Plot of the time dependence of absorbance at 588 nm for the formation of bromophenol blue in the reaction of $MoO(O_2)_2(C_2O_4)^{2-}$, H_2O_2, Br^-, and phenol red at 25 °C. Initial concentrations: 1 mM $MoO(O_2)_2(C_2O_4)^{2-}$; 1 mM H_2O_2; 0.025 M LiBr; 4.5×10^{-5} M phenol red; 0.010 M oxalate buffer (pH 5.0); 1.0 M ionic strength.

at pH 5.0. The maximum at 432 nm characteristic of phenol red disappeared in favor of the peak at 588 nm due to bromophenol blue. The time dependence for the absorbance at 588 nm for the same experiment appears in Figure 5. The duration of the initial lag decreased with increasing $MoO(O_2)_2(C_2O_4)^{2-}$ or bromide concentration. The significance of this lag phase is discussed below. Systematic variation of initial concentrations and measurement of the initial rate dA_{588}/dt from the slope of the linear portion of the absorbance vs time curves (supplementary Table S1) permitted determination of the order of the reaction with respect to each reactant. The variation of dA_{588}/dt with initial concentration was linear for $MoO(O_2)_2(C_2O_4)^{2-}$ (0.1–1 mM, correlation coefficient = 0.999 for three points) and bromide (0.025–0.500 M, correlation coefficient = 1.000 for six points), indicating a first-order dependence of the initial rate on these reactants. The initial rate was independent of changes in the initial concentration of hydrogen peroxide (1–10 mM, average $dA_{588}/dt = (4.1 \pm 0.3) \times 10^{-2}$ s^{-1} for four points) and phenol red ($(1-5) \times 10^{-5}$ M, average $dA_{588}/dt = (1.39 \pm 0.08) \times 10^{-2}$ s^{-1} for five points), where the uncertainty is the standard deviation. The second-order rate law

for the formation of bromine is given in eq 3. The absolute

$$d[Br^+]/dt = k_{Br}[MoO(O_2)_2(C_2O_4)^{2-}][Br^-] \quad (3)$$

reaction rate $d[Br^+]/dt$ was obtained from the experimental quantity dA_{588}/dt by use of eq 4. The factor $d[Br^+]/dA$ is the

$$d[Br^+]/dt = (dA_{588}/dt)(d[Br^+]/dA) \quad (4)$$

reciprocal of the slope of a plot of absorbance at 588 nm vs $[Br^+]$ for a series of standardized bromine solutions combined with 4.5×10^{-5} M phenol red and excess bromide. The value $dA/d[Br^+] = 15\,800\ M^{-1}$ was obtained at pH 5.0 in both oxalate and acetate buffer, at 0.025 and 0.500 M bromide. This factor and eqs 3 and 4 permit the calculation of the second-order rate constant k_{Br} for each experiment. The average value is $k_{Br} = (4.8 \pm 0.4) \times 10^{-3}\ M^{-1}\ s^{-1}$ for the formation of bromine by this system at pH 5.0 and 1.0 M ionic strength. The uncertainty is the standard deviation of the average of 16 values.

For comparison, the reactivity of bromide with $MoO(OH)(O_2)_2(H_2O)^-$ was briefly investigated. Systematic variation of initial concentrations and measurement of the initial rate of bromophenol blue formation (data not shown) showed the reaction to be first-order in molybdenum complex and zeroth-order in hydrogen peroxide. The dependence of the initial rate on bromide was first-order at low initial concentrations but more complicated at higher concentrations. From the data obtained at low initial bromide concentrations, we estimate a second-order rate constant $k_{Br} \cong 3 \times 10^{-4}\ M^{-1}\ s^{-1}$ at pH 5.0 and 1.0 M ionic strength for the oxidation of bromide by $MoO(OH)(O_2)_2(H_2O)^-$.

The complex $WO(O_2)_2(C_2O_4)^{2-}$ was prepared in situ for subsequent reaction with bromide. In the presence of 20 mM hydrogen peroxide and 0.010 M oxalate buffer, 0.1 mM tungstate ion oxidized bromide at a faster rate than did an equivalent concentration of $MoO(O_2)_2(C_2O_4)^{2-}$, but at least two catalytic species were evident. Our efforts to obtain solutions in which $WO(O_2)_2(C_2O_4)^{2-}$ predominates have been unsatisfactory.

Uncatalyzed Bromide Oxidation. The very slow oxidation of bromide by hydrogen peroxide in the absence of a metal catalyst was followed at pH 5.0 (acetate buffer) and 1.0 M ionic strength by monitoring the bromination of phenol red. A first-order dependence on bromide concentration was apparent, but the dependence on hydrogen peroxide over the range 10−200 mM was more complicated. For low hydrogen peroxide concentrations, however, the reaction was assumed to be first-order in H_2O_2, and an upper limit for the rate constant for the rate law $d[Br^+]dt = k_{un}[H_2O_2][Br^-]$ was estimated as $k_{un} = 6 \times 10^{-7}\ M^{-1}\ s^{-1}$.

Product Yield. The quantity of bromine produced by the reaction of a mixture of 1.0 mM $MoO(O_2)_2(C_2O_4)^{2-}$, 5.0 mM H_2O_2, and 1.0 M LiBr in the presence of 1.9×10^{-3} M phenol red and 0.040 M oxalate buffer (pH 5.0) was determined by spectrophotometric measurement of bromophenol blue at 588 nm over a 51-h period. The filled circles in Figure 6 represent the catalyzed case, while the open circles stand for the analogous experiment without $MoO(O_2)_2(C_2O_4)^{2-}$. From a total peroxide concentration of 7.0 mM, a bromine concentration of 5.8 mM was generated. This value was typical of those obtained in several replicate determinations.

Oxygen Evolution. In the absence of an organic substrate, dioxygen was evolved by the reaction mixture. To solutions initially containing 67 μM MoO_4^{2-}, 0.033 M LiBr, and 0.010 M oxalate buffer (pH 5.0) were added small volumes of hydrogen peroxide solution to initiate formation of the

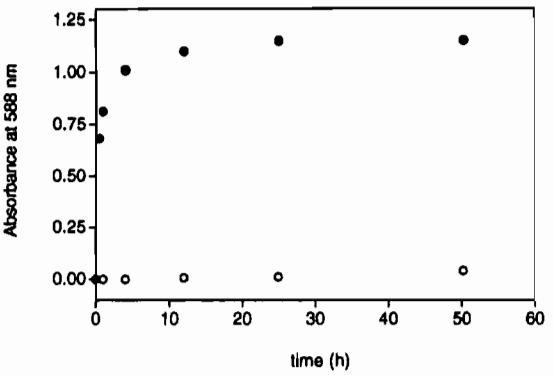

Figure 6. Time dependence of the production of bromophenol blue from phenol red for the catalyzed (filled circles) and uncatalyzed (open circles) oxidation of bromide by H_2O_2. Each point represents an 80-fold dilution in 0.010 M oxalate buffer (pH 5.0) of the reaction mixture, which initially contained 1.0 mM (filled) or 0 mM (open) $MoO(O_2)_2(C_2O_4)^{2-}$, 5.0 mM H_2O_2, 1.0 M LiBr, 1.8×10^{-3} M phenol red, and 0.040 M oxalate buffer at pH 5.0.

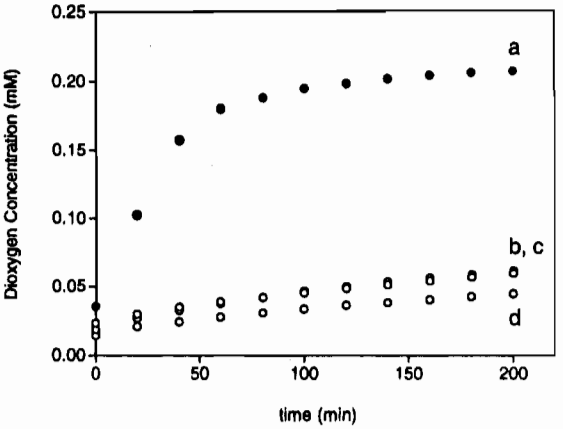

Figure 7. Time dependence of dioxygen formation in the reaction of $MoO(O_2)_2(C_2O_4)^{2-}$, H_2O_2, and Br^-. Conditions: (a) $MoO_4^{2-} + H_2O_2 + Br^- +$ oxalate; (b) $MoO_4^{2-} + H_2O_2 + Br^- +$ oxalate + phenol red; (c) $H_2O_2 + Br^- +$ oxalate; (d) $MoO_4^{2-} + H_2O_2 +$ oxalate. Initial conditions, where applicable, were 0.134 mM MoO_4^{2-}, 0.40 mM H_2O_2, 1.0 M LiBr, 1.1×10^{-4} M phenol red, and 0.040 M oxalate buffer at pH 5.0. In (d), ionic strength was adjusted to 1.0 M with $LiClO_4$.

$MoO(O_2)_2(C_2O_4)^{2-}$ complex[29] and subsequent reaction with bromide. Essentially identical initial rates $d[O_2]/dt = 0.59$ μM/min ($[H_2O_2]_0 = 2.0$ mM) and 0.64 μM/min ($[H_2O_2]_0 = 4.0$ mM) were obtained, indicating that oxygen production is independent of the initial peroxide concentration. Quantitation of the O_2 produced was achieved with lower initial concentrations of hydrogen peroxide. Figure 7a illustrates the production of O_2 over time for a solution containing 67 μM MoO_4^{2-}, 2.0 M LiBr, 0.010 M oxalate buffer (pH 5.0), and 0.4 mM H_2O_2. The total oxygen production represented by Figure 7a is ca. 0.17 mM, or 86% of the expected value of 0.20 mM. The remaining oxygen was presumably lost by diffusion from the cell during the relatively long reaction time. Also shown in Figure 7 are traces demonstrating that dioxygen is not evolved in the presence of phenol red (b), in the absence of catalyst (c), or in the absence of bromide (d).

$VO(O_2)_2(C_2O_4)^{3-}$. The aqueous chemistry of vanadium(V) with peroxide and oxalate ligands is more complicated than that of the molybdenum(VI) system. The ^{51}V NMR spectra of solutions prepared with $VO(O_2)_2(C_2O_4)^{3-}$ and varying concentrations of hydrogen peroxide and oxalate buffer at pH 5.0 showed $VO(O_2)_2(H_2O)_2^-$ (−690 ppm) to be the principal species at low oxalate concentrations and $VO(O_2)(C_2O_4)_2^{3-}$ (−597 ppm) to predominate at high oxalate concentrations. A signal assigned

to $VO(O_2)_2(C_2O_4)^{3-}$ was observed at −737 ppm, but in no case was this complex obtained as the predominant species.

According to the ^{51}V NMR spectrum, a solution containing 1 mM $VO(O_2)_2(C_2O_4)^{3-}$, 1 mM H_2O_2, and 10 mM oxalate buffer (pH 5.0) consisted primarily of $VO(O_2)(C_2O_4)_2^{3-}$. In the presence of 4.5×10^{-5} M phenol red, 0.400 M LiBr, and sufficient $LiClO_4$ to adjust the ionic strength to 1.0 M, the solution exhibited a rate of bromophenol blue production from phenol red that was indistinguishable from the uncatalyzed rate of bromide oxidation by hydrogen peroxide.

Discussion

Several factors influence the integrity of the starting $MoO(O_2)_2(C_2O_4)^{2-}$ complex in these reactions. Molybdate complexes with oxalate ligand have been shown by Cruywagen et al. to be monomeric at pH 5.0 at concentrations up to 50 mM.[50] Oxalate buffer is required to prevent the dissociation of the oxalate ligand from the $MoO(O_2)_2(C_2O_4)^{2-}$ complex. When $MoO(O_2)_2(C_2O_4)^{2-}$ is dissolved in acetate buffer at pH 5.0, the spectrum of $MoO(OH)(O_2)_2(H_2O)^-$ (λ_{max} = 310 nm)[29] is obtained, but in oxalate buffer at pH 5.0, the characteristic maximum absorbance at 320 nm for $MoO(O_2)_2(C_2O_4)^{2-}$ is observed. The formation constant for $MoO_3(C_2O_4)^{2-}$ according to eq 5 is 4.2×10^{13}, as reported by Cruywagen et al. Ghiron

$$MoO_4^{2-} + C_2O_4^{2-} + 2H^+ \rightleftharpoons MoO_3(C_2O_4)^{2-} + H_2O \quad (5)$$

and Thompson provide an equilibrium constant of 2.6×10^7 (determined at pH 4.0) for the formation of $MoO(O_2)_2(C_2O_4)^{2-}$ from $MoO_3(C_2O_4)^{2-}$ and hydrogen peroxide, as written in eq 6.[29] Equation 7 describes the formation of the unchelated

$$MoO_3(C_2O_4)^{2-} + 2H_2O_2 \rightleftharpoons MoO(O_2)_2(C_2O_4)^{2-} + 2H_2O \quad (6)$$

$$MoO_4^{2-} + 2H_2O_2 + H^+ \rightleftharpoons MoO(OH)(O_2)_2(H_2O)^- + H_2O \quad (7)$$

$MoO(OH)(O_2)_2(H_2O)^-$, for which an equilibrium constant of 6×10^8 has been measured at pH 4.0.[29] From these data we calculate an equilibrium constant of 2×10^{12} for the formation of $MoO(O_2)_2(C_2O_4)^{2-}$ from $MoO(OH)(O_2)_2(H_2O)^-$, as shown in eq 8. Application of these equilibrium constants to a solution

$$MoO(OH)(O_2)_2(H_2O)^- + C_2O_4^{2-} + H^+ \rightleftharpoons MoO(O_2)_2(C_2O_4)^{2-} + 2H_2O \quad (8)$$

of $MoO(O_2)_2(C_2O_4)^{2-}$ in 0.010 M oxalate buffer solution at pH 5.0, for which the free $C_2O_4^{2-}$ concentration is 8.6×10^{-3} M, yields a ratio of $MoO(O_2)_2(C_2O_4)^{2-}$ to $MoO(OH)(O_2)_2(H_2O)^-$ of greater than 150 000 to 1.

Exogenous hydrogen peroxide is required to maintain the molybdenum oxalate complex in the diperoxo form. Ghiron and Thompson have estimated a value of $K = 17$ for eq 9, in

$$MoO_3(C_2O_4)^{2-} + H_2O_2 \rightleftharpoons MoO_2(O_2)(C_2O_4)(H_2O)^{2-} \quad (9)$$

which a monoperoxo species formulated as $MoO_2(O_2)(C_2O_4)(H_2O)^{2-}$ is formed from the reaction between $MoO_3(C_2O_4)^{2-}$ and hydrogen peroxide.[29] From eqs 6 and 9, we calculate an equilibrium constant of about 7×10^{-7} for the loss of a peroxo ligand from the diperoxomolybdenum complex

(50) Cruywagen, J. J.; Heyns, J. B.; van de Water, R. F. *J. Chem. Soc., Dalton Trans.* **1986**, 1857–1862.

Scheme 1

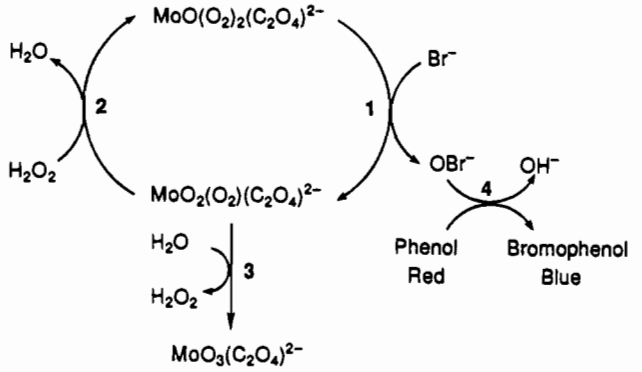

to give the monoperoxo complex (eq 10). The lowest hydrogen

$$MoO(O_2)_2(C_2O_4)^{2-} + 2H_2O \rightleftharpoons MoO_2(O_2)(C_2O_4)(H_2O)^{2-} + H_2O_2 \quad (10)$$

peroxide concentration employed in our experiments was 1 mM, in conjunction with a $MoO(O_2)_2(C_2O_4)^{2-}$ concentration of 1 mM. At these levels, the initial ratio of diperoxo to monoperoxo complex was more than 1400 to 1. Higher ratios prevailed in the experiments involving larger concentrations of hydrogen peroxide. The effect of hydrogen peroxide consumption during the course of the reaction on the conversion between the di- and monoperoxo complexes will be discussed below.

The catalytic cycle presented in Scheme 1 satisfactorily describes the principal features of our data. Step 1 involves the rate-limiting reaction of $MoO(O_2)_2(C_2O_4)^{2-}$ and bromide to yield bromine in an oxidized form (shown here as hypobromite) and an intermediate postulated as a dioxo monoperoxo complex of molybdenum(VI) and the oxalate anion. This intermediate combines with hydrogen peroxide to regenerate the starting $MoO(O_2)_2(C_2O_4)^{2-}$ (step 2) or undergoes hydrolysis to yield the $MoO_3(C_2O_4)^{2-}$ product (step 3). In step 4, an organic substrate, shown here as phenol red, is brominated. Steps 2 and 3 are reversible, but this model treats only the kinetically important processes.

That step 2 is faster than step 1 is demonstrated by the zeroth-order dependence of the overall reaction on hydrogen peroxide concentration. The rapid reaction of the monoperoxo intermediate with hydrogen peroxide to regenerate $MoO(O_2)_2(C_2O_4)^{2-}$ (step 2) and the hydrolysis of the intermediate to give $MoO_3(C_2O_4)^{2-}$ (step 3) prevent the accumulation of the intermediate species and result in the persistence of only the initial $MoO(O_2)_2(C_2O_4)^{2-}$ and final $MoO_3(C_2O_4)^{2-}$ species, consistent with our observation of an isosbestic point (Figure 1). The establishment of the isosbestic point also implies that oxidized bromine makes no contribution to the absorbance of the solution under conditions of low initial bromide concentration.

The rapid regeneration of the starting $MoO(O_2)_2(C_2O_4)^{2-}$ complex from the monoperoxo intermediate and hydrogen peroxide accounts for the lag observed in the disappearance of $MoO(O_2)_2(C_2O_4)^{2-}$. Increasing the initial concentration of hydrogen peroxide increases the rate of step 2, resulting in the persistence of the diperoxo complex for increasingly longer times (Figure 2).

That bromide is oxidized by this system is confirmed by the bromination of phenol red to bromophenol blue (Figure 4). Very early in the reaction, the concentration of OBr^- is small and the bromination of phenol red is slow, producing a lag in the data (Figure 5). When sufficient OBr^- has been produced to

achieve a steady-state concentration, the rate of production of bromophenol blue is equal to the rate of oxidized bromine formation by the $MoO(O_2)_2(C_2O_4)^{2-}$ catalyst. The growth of a feature between 560 and 580 nm at early times in Figure 4 suggests the initial formation of dibromophenol red,[47] but by the end of the lag phase only bromophenol blue (588 nm) is in evidence. Knowledge of the exact mechanism of phenol red bromination is not critical to our analysis because initial rates were measured from the linear portion of the trace, where only the tetrabrominated product was observed. The value $dA/d[Br^+] = 15\,800\ M^{-1}$ corresponds to an effective molar absorptivity of 63 100 $M^{-1}\ cm^{-1}$ for the bromophenol blue product. The molar absorptivity at 588 nm of an authentic sample of bromophenol blue was 62 900 $M^{-1}\ cm^{-1}$ at pH 5.0 and 1.0 M ionic strength.[51] The close agreement between the values indicates that tetrabromination of phenol red is quantitative.

The bromination of phenol red to yield bromophenol blue was previously reported as an analysis for bromine in seawater[45] and as an assay for bromoperoxidase activity.[48] Our demonstration that the initial rate of bromophenol blue production is independent of phenol red concentration establishes that the tetrabromination process is sufficiently rapid to be used in the measurement of bromine production by this system. The use of this method is limited to pH values close to 5.0 in order to achieve a transformation from the yellow form of phenol red ($pK_a = 7.9$) to the blue form of bromophenol blue ($pK_a = 4.0$).

The reaction of bromine with phenol red was faster than the reaction of bromine with oxalate, as shown by the identical values of $dA/d[Br^+]$ in oxalate and acetate buffers. Interference from oxalate in the measurement of bromine production was therefore disregarded. Furthermore, the value of $dA/d[Br^+]$ was the same whether measured under conditions of low bromide concentration, where Br_2 predominates at this pH, or at high bromide concentration, where Br_3^- is the principal species.

Application of the steady-state approximation to the intermediate species $MoO_2(O_2)(C_2O_4)^{2-}$ permits the derivation of a rate law for Scheme 1 in terms of the disappearance of the starting complex $MoO(O_2)_2(C_2O_4)^{2-}$, as shown in eq 11.

$$-d[MoO(O_2)_2(C_2O_4)^{2-}]/dt = k_1\left(\frac{k_3}{k_2[H_2O_2] + k_3}\right)[MoO(O_2)_2(C_2O_4)^{2-}][Br^-] \quad (11)$$

If the rate of bromophenol blue production under steady-state conditions is taken to be the rate of oxidized bromine production,[52] then the rate law for Scheme 1 in terms of bromine production can be written as the second-order equation (12).

$$d[Br^+]/dt = k_1[MoO(O_2)_2(C_2O_4)^{2-}][Br^-] \quad (12)$$

Equation 12 is equivalent to eq 3, and thus k_1 is identical with k_{Br}, obtained from the rate of production of bromine. Comparison of eqs 11 and 12 reveals the difference between k_{Mo} ($2.3 \times 10^{-3}\ M^{-1}\ s^{-1}$), obtained from the rate of disappearance of $MoO(O_2)_2(C_2O_4)^{2-}$, and k_{Br} ($4.8 \times 10^{-3}\ M^{-1}\ s^{-1}$). Equation 11 is identical with eq 12 only when $[H_2O_2] = 0$; otherwise, even for very small concentrations of hydrogen peroxide, the effective rate constant for eq 11 is less than k_1, consistent with a value of k_{Mo} less than that of k_{Br}. The partitioning ratio $k_3/(k_2[H_2O_2] + k_3)$ in eq 11 represents the probability that, at the branch point of the mechanism, hydrolysis will occur in favor of regeneration of the starting complex. The value of this partitioning ratio can be estimated as $k_{Mo}/k_{Br} \cong 0.5$ and suggests that for every intermediate species completing the cycle in step 2, one is hydrolyzed to $MoO_3(C_2O_4)^{2-}$ (step 3). The rate of hydrogen peroxide consumption is thus equal to the rate of hydrogen peroxide production, implying a steady-state situation for hydrogen peroxide during the latter phase of the reaction under these conditions. A small but constant hydrogen peroxide concentration for this portion of the reaction justifies the designation of k_{Mo} as a rate *constant* and renders eqs 2 and 11 identical. Further, this analysis shows the necessity of measuring the kinetics of this system by following the production of bromine rather than the disappearance of $MoO(O_2)_2(C_2O_4)^{2-}$, since it is k_{Br} that corresponds directly to the rate-limiting step of the process.

Although hydrogen peroxide is required initially to maintain the molybdenum complex in the diperoxo form, the diminution of H_2O_2 during the course of the reaction does not lead to hydrolysis of the remaining diperoxo species. The pseudo-first-order reaction of $MoO(O_2)_2(C_2O_4)^{2-}$ with excess bromide is faster than its hydrolysis to the monoperoxo species, as indicated by the isosbestic point. If the reaction of water with $MoO(O_2)_2(C_2O_4)^{2-}$ to give $MoO_2(O_2)(C_2O_4)^{2-}$ and H_2O_2 were competitive in rate with the reaction between $MoO(O_2)_2(C_2O_4)^{2-}$ and excess bromide, the accumulation of the monoperoxo intermediate would prevent the establishment of an isosbestic point.

Furthermore, the presence of isosbestic point reveals that there is no significant accumulation of Br^+ in solution. In the absence of an organic substrate, the nascent Br^+ is reduced by hydrogen peroxide (see below), and at low initial concentrations of bromide, the rate of Br^+ production in step 1 is sufficiently slow that the steady-state concentration of Br^+ is negligible. The isosbestic point is destroyed at higher bromide concentrations, and in the extreme cases a transient species characteristic of tribromide ($\lambda_{max} = 265$ nm)[46] is observed. Increasing the bromide concentration permits the accumulation of tribromide by (1) increasing the rate of step 1 and (2) slowing the rate of Br^+ reduction by hydrogen peroxide (see below) by increasing the concentration of Br_3^- relative to the more reactive HOBr and Br_2.[53]

The reduction of oxidized bromine by hydrogen peroxide to yield bromide and dioxygen is generalized in eq 13. The

$$H_2O_2 + Br^+ \rightarrow O_2 + Br^- + 2H^+ \quad (13)$$

mechanism of this process is not well understood, although an early study implicates HOBr as the primary reactive species with peroxide.[53] The independence of the initial rate of dioxygen production, $d[O_2]/dt$, on hydrogen peroxide concentration indicates that eq 13 is not the rate-limiting step of the catalytic cycle in the absence of substrate. The net process of bromide oxidation by H_2O_2 and subsequent bromine reduction by H_2O_2 has been summarized as the bromide-assisted disproportionation of H_2O_2[36] and is observed to occur for vanadium bromoperoxidase in the absence of an organic substrate.[54,55]

The site of bromide attack on the diperoxomolybdenum complex may be a peroxo ligand, the metal center itself, or, improbably, the terminal oxo ligand. We discount direct binding of bromide to molybdenum because of the tightly chelating oxalate ligand and the requirement that molybdenum expand

(51) $\epsilon = 67\,400\ M^{-1}\ s^{-1}$ at 592 nm for pH 6.5 and unspecified ionic strength.[46]

(52) The stoichiometric factor of 4 for the tetrabromination is included in the factor $d[Br^+]/dA$ used in the conversion of dA_{588}/dt to $d[Br^+]/dt$.

(53) Bray, W. C.; Livingston, R. C. *J. Am. Chem. Soc.* **1928**, *50*, 1654–1665.
(54) Everett, R. R.; Butler, A. *Inorg. Chem.* **1989**, *28*, 393–395.
(55) Manthey, J. A.; Hager, L. P. *J. Biol. Chem.* **1981**, *256*, 11232–11238.

its coordination number to 8. This argument is supported by our finding that the rate of bromide oxidation by the chelated $MoO(O_2)_2(C_2O_4)^{2-}$ is an order of magnitude faster than that effected by the more accessible $MoO(OH)(O_2)_2(H_2O)^-$ at pH 5.0 and 1.0 M ionic strength. The reverse would be expected if coordination of bromide to the metal center were involved. Ghiron and Thompson reached a similar conclusion for the oxidation of $Co(en)_2(SCH_2CH_2NH_2)^{2+}$ by these complexes upon finding that at pH 4.0 the rate for $MoO(O_2)_2(C_2O_4)^{2-}$ was about 10 times faster than that for $MoO(OH)(O_2)_2(H_2O)^-$.[29]

The monoperoxo intermediate invoked in Scheme 1 has precedent in the mechanism proposed by Ghiron and Thompson for the $MoO(O_2)_2(C_2O_4)^{2-}$-catalyzed oxidation of the coordinated thiolate ligand in $Co(en)_2(SCH_2CH_2NH_2)^{2+}$.[29] The mechanism of Scheme 1 posits the reaction of bromide with the diperoxo complex and not with the monoperoxo intermediate. Were bromide to react with both the diperoxo and the monoperoxo species, the first-order dependence of the experimental rate law on bromide would require the monoperoxo species to react faster than the diperoxo species. We assume that the rate of interaction between bromide and the monoperoxo species is negligible because (1) the concentration of the monoperoxo species is extremely small and (2) monoperoxo metal species were shown in several instances to be less reactive in aqueous solution than their diperoxo counterparts.[29,30] Our observation that $VO(O_2)(C_2O_4)_2^{3-}$ oxidizes bromide at a rate indistinguishable from that of the uncatalyzed case is consistent with this trend.

Griffith and co-workers[20] described the disproportionation of the monoperoxo complex $MoO_2(O_2)(C_2O_4)(H_2O)^{2-}$ to $MoO(O_2)_2(C_2O_4)^{2-}$ and $MoO_3(C_2O_4)^{2-}$ according to eq 14. Such an

$$2MoO_2(O_2)(C_2O_4)(H_2O)^{2-} \rightleftharpoons MoO(O_2)_2(C_2O_4)^{2-} + MoO_3(C_2O_4)^{2-} + 2H_2O \quad (14)$$

interconversion may occur in the present bromide oxidation system, in addition to the processes indicated in Scheme 1.

The rate constant for the oxidation of $Co(en)_2(SCH_2CH_2NH_2)^{2+}$ by $VO(O_2)_2(C_2O_4)^{3-}$ in acetate buffer at pH 5.1 and 20.6 °C was reported as $k = 12\ M^{-1}\ s^{-1}$, while the value for this oxidation by $VO(O_2)_2(H_2O)_2^-$ was $k = 11\ M^{-1}\ s^{-1}$ (25 °C).[30] We examined a $VO(O_2)_2(C_2O_4)^{3-}$ solution of the same concentrations (0.36 mM $VO(O_2)_2(C_2O_4)^{3-}$, 1.8 mM H_2O_2, and 10.0 mM acetate buffer (pH 5.0)) by ^{51}V NMR spectroscopy and found $VO(O_2)_2(H_2O)_2^-$ (−690 ppm) as the sole vanadium species. Quilitzsch and Wieghardt described the rapid, acid-catalyzed hydrolysis of several diperoxovanadate complexes and a subsequent, slower decomposition that presumably involved the loss of the organic ligand from the monoperoxo species.[56] Although our experiments were performed at lower acid concentration, we employ the rate constant expression of Quilitzsch and Wieghardt to estimate that the half-life for hydrolysis of the first peroxo ligand in a $VO(O_2)_2(C_2O_4)^{3-}$ solution containing 1×10^{-5} M H^+ and 1.8 mM H_2O_2 is about 13 s. Since our ^{51}V NMR experiments were performed at least 5 min after solution preparation, it is reasonable to suppose that hydrolysis and dissociation of the oxalato ligand occurred during this time. It should be noted that oxalate buffer was not employed to counteract the dissociation of the oxalato ligand. The equilibrium constant for the interconversion of diperoxo and monoperoxo aqua complexes, shown in eq 15 with water

$$VO(O_2)^+ + H_2O_2 \rightleftharpoons VO(O_2)_2^- + 2H^+ \quad (15)$$

ligands omitted, is $K = 0.6$ at 25 °C and 0.3 M ionic strength.[57] At pH 5.0 and 1.8 mM H_2O_2, the diperoxo species is favored over the monoperoxo species by a factor of about 10^7. It is therefore not surprising that only $VO(O_2)_2(H_2O)_2^-$ was observed in the NMR experiment. Furthermore, it is possible that the rate constants reported for the oxidation of $Co(en)_2(SCH_2CH_2NH_2)^{2+}$ by $VO(O_2)_2(C_2O_4)^{3-}$ and $VO(O_2)_2(H_2O)_2^-$ were identical because $VO(O_2)_2(H_2O)_2^-$ was the oxidant in both cases.

We estimate an upper limit to the rate constant for the uncatalyzed oxidation of bromide by hydrogen peroxide as $k_{un} = 6 \times 10^{-7}\ M^{-1}\ s^{-1}$ at 25 °C, pH 5.0, and 1.0 M ionic strength. Equation 16 defines the rate expression reported for this process

$$-d[H_2O_2]/dt = (k_a + k_b[H^+])[H_2O_2][Br^-] \quad (16)$$

at 25 °C and 0.40 M ionic strength, where $k_a = 3.8 \times 10^{-7}\ M^{-1}\ s^{-1}$ and $k_b = 2.3 \times 10^{-4}\ M^{-2}\ s^{-1}$.[58] The effective second-order rate constant calculated from eq 16 for pH 5.0 is $k_{un} = 3.8 \times 10^{-7}\ M^{-1}\ s^{-1}$, in good agreement with our value.

With $k_{Br} = 4.8 \times 10^{-3}\ M^{-1}\ s^{-1}$, $MoO(O_2)_2(C_2O_4)^{2-}$ has a reactivity 8000 times that of H_2O_2, and the tungsten analogue is estimated to be even more reactive. Similar results were reported by Ghiron and Thompson for the oxidation of $Co(en)_2(SCH_2CH_2NH_2)^{2+}$ by diperoxo metal species containing coordinated water molecules. They found that the reactivities of H_2O_2, V(V), Mo(VI), and W(VI) have the ratio $1:10:10^4:10^5$, but they noted that the complexes lack dramatic structural differences to which the reactivity differences can be attributed.[30]

Conclusions

The coordination of peroxide to molybdenum(VI) in the complex $MoO(O_2)_2(C_2O_4)^{2-}$ activates peroxide toward oxidation of bromide by a factor of 8000 over free peroxide at pH 5.0. The rate-determining step is a bimolecular interaction between the metal complex and bromide. A catalytic mechanism implicating a monoperoxo intermediate satisfactorily explains the experimental results. The bromination of phenol red to yield bromophenol blue is an effective means of quantifying the rate of bromine production. Efforts to elucidate the molecular details of the interaction between bromide and peroxometal complexes and to determine the influence of the chelating ligand on complex reactivity are in progress.

Acknowledgment. This research was supported by a Joseph H. DeFrees Grant from the Research Corp., by the donors of the Petroleum Research Fund, administered by the American Chemical Society, and by NSF-REU Grants CHE-9300589 and CHE-9200358. We thank Prof. Alison Butler for use of the oxygen electrode, Prof. Roger Rowlett and Ms. Melissa Clague for helpful discussions, and Ms. Julie Brown for the initial tungsten experiments.

Supplementary Material Available: A table giving kinetics results for bromophenol blue formation (1 page). Ordering information is given on any current masthead page.

(56) Quilitzsch, U.; Wieghardt, K. *Inorg. Chem.* **1979**, *18*, 869−871.

(57) Secco, F. *Inorg. Chem.* **1980**, *19*, 2722−2725.

(58) Mohammad, A.; Liebhafsky, H. A. *J. Am. Chem. Soc.* **1934**, *56*, 1680−1685.